ISSN 1674-1056
http://cpb.iphy.ac.cn
http://iopscience.iop.org/cpb
中国物理 B
Chinese Physics
中国物理
Chinese Physics B

Strong coupling between height of gaps and thickness of thermal boundary layer in partitioned convection system

Ze-Peng Lin(林泽鹏), Yun Bao(包芸)
Citation: Chin. Phys. B . 2019, 28(9): 094701 . **doi:** 10.1088/1674-1056/28/9/094701
Journal homepage: http://cpb.iphy.ac.cn; http://iopscience.iop.org/cpb

What follows is a list of articles you may be interested in

Numerical study of heat-transfer in two-and quasi-two-dimensional Rayleigh-Bénard convection

Zhen-Yuan Gao(高振源), Jia-Hui Luo(罗嘉辉), Yun Bao(包芸)
Chin. Phys. B . 2018, 27(10): 104702 . **doi:** 10.1088/1674-1056/27/10/104702

Analytical study of Cattaneo-Christov heat flux model for a boundary layer flow of Oldroyd-B fluid

F M Abbasi, M Mustafa, S A Shehzad, M S Alhuthali, T Hayat
Chin. Phys. B . 2016, 25(1): 014701 . **doi:** 10.1088/1674-1056/25/1/014701

Heat transfer analysis in the flow of Walters'B fluid with a convective boundary condition

T. Hayat, Sadia Asad, M. Mustafa, Hamed H. Alsulami
Chin. Phys. B . 2014, 23(8): 084701 . **doi:** 10.1088/1674-1056/23/8/084701

Boundary layer flow and heat transfer of a Casson fluid past a symmetric porous wedge with surface heat flux

Swati Mukhopadhyay, Iswar Chandra Mandal
Chin. Phys. B . 2014, 23(4): 044702 . **doi:** 10.1088/1674-1056/23/4/044702

Strong coupling between height of gaps and thickness of thermal boundary layer in partitioned convection system*

Ze-Peng Lin(林泽鹏) and Yun Bao(包芸)†

Department of Mechanics, Sun Yat-Sen University, Guangzhou 510275, *China*

(Received 14 April 2019; revised manuscript received 3 June 2019; published online 23 August 2019)

A direct numerical simulation (DNS) method is used to calculate the partitioned convection system with *Ra* number ranging from 10^7 to 2×10^9. Using the boundary layer thickness to normalize the height of gaps d, we find a strong consistency between the variation of the TD number (the average value of the temperature in each heat transfer channel is averaged after taking the absolute values) with the change of the height of gaps and the variation of the TD number with the change of *Ra* number in partitioned convection. For a given thickness of partition, heights of gaps are approximately equal to 0.5 or 1 time of the thermal boundary layer thickness λ_θ at different *Ra* numbers. TD number representing temperature characteristics is almost the constant value, which means that TD number is a function of d/λ_θ only. Analysis of local temperature field of area in gaps shows that the temperature distribution in the gaps are basically the same when d/λ_θ is certain. The heat transfer *Nu* number of the system at $d/\lambda_\theta \approx 0.5$ is larger than that of $d/\lambda_\theta \approx 1$, both of them have the same scaling law with *Ra* number and $Nu \sim Ra^{0.25}$.

Keywords: partitioned convection system, height of gaps, thermal boundary layer, TD number

PACS: 47.27.te **DOI:** 10.1088/1674-1056/ab343d

1. Introduction

Thermal convection is widespread in nature and daily life, which has drawn great focus among researchers.[1,2] Rayleigh-Bénard (RB) convection is a classical physical model in the field of natural convection research,[3] and heat transfer enhancement is one of the hot spots in such field.[4] In recent years, a rising amount of studies have focused on the non-standard RB convection. Compared with the standard RB convection system, it was found by experiments and numerical simulations that some non-standard RB thermal convection systems can enhance heat transfer efficiency, such as RB convection with rough plates,[5–7] corilois force,[8–10] with phase transition,[11] with polymer addition,[12,13] partitions.[14–18] There are both passive and active ways to improve the heat transfer efficiency. Due to the fact that the passive method does not introduce external powers, it has been widely concerned and deeply studied for a long time. However, the heat transfer enhancement is generally less than one time.[19–21]

As a passive method, the partitioned convection system has achieved an extraordinary heat transfer enhancement. Bao *et al.*[14] added vertical partitions at equal distances in the RB convection devices with aspect ratio of 5, and left gaps at both ends of the partitions away from the top and bottom plates. It was found that the heat transfer efficiency increased significantly while the number of partitions increases. Through numerical simulation, Bao *et al.*[15] found that when the number of partitions increased to 28, adjusting the height of gaps can further improve the heat transfer efficiency, which was excited up to 3.1 times that of the non-partition device. Lin *et al.*[16] further studied the influence of different geometrical parameters on the flow and heat transfer characteristics of the system, and found that the height of gaps is the key geometric parameter in the partitioned convection system. Lin and Bao[17] focused on the TD number, representing the strength of heat separation in this system, and found that TD reflects the magnitude of buoyancy, which is balanced by the pressure difference ΔP between the top and bottom of the heat transfer channels. In addition, there is a scale relation with exponent -1.64 between TD and the height of gaps in a certain range,[17] and a scale relation with exponent 0.4 between TD and *Ra*.[18] Therefore, in this paper, size of TD number will be concerned when the temperature characteristics of systems are studied.

In the partitioned convection system, the height of gaps is usually chosen on the same order of magnitude as the thickness of thermal boundary layer. The change of the thickness of the thermal boundary layer of the RB convection system under different *Ra* numbers is based on a certain law. In this paper, the height of gaps of the partitioned convection system is related to the thickness of the thermal boundary layer of RB convection system, and the temperature characteristics and heat transfer characteristics of the partitioned convection system are discussed when the ratio of height of gaps to thickness of boundary layer takes some specific values.

*Project supported by the National Natural Science Foundation of China (Grant Nos. 11772362 and 11452002) and the Special Scientific Research Fund for Super Computing in the Joint Fund of the National Natural Science Foundation of China and the People's Government of Guangdong Province, China (Phase II, nsfc2015_570).

†Corresponding author. E-mail: stsby@mail.sysu.edu.cn

© 2019 Chinese Physical Society and IOP Publishing Ltd

2. Numerical methods

RB convection is an enclosed system with fluid heated from the bottom and cooled from the top. The convective cavity has height H, width D, and thickness W. We consider an RB convection system with vertical partitions equally distributed in the cell. As illustrated in Fig. 1(a), the partitions are connected with the front and back sidewalls. Both ends are kept away from the cooling and heating plates in a distance d. Figure 1(b) is a zoom-in view of the convective cell. Here l represents the thickness of the partitions and b the width of the vertical channels.

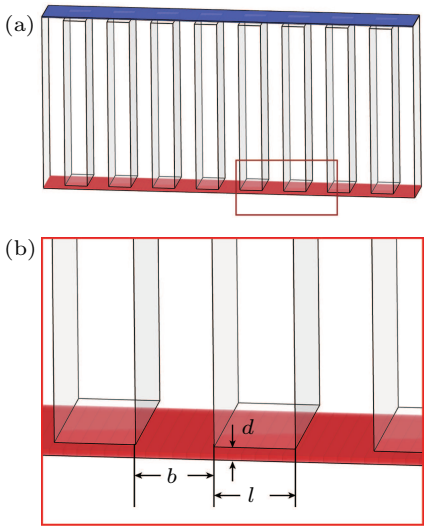


Fig. 1. (a) The model diagram of partition convection device. (b) An enlarged portion of the partition convection device.

Previous studies have shown that when the number of partitions is large enough, the flows in the channels will become laminar. In such case, the heat transfer efficiency will be the same for both two- and three-dimensional partitioned RBC systems.[15] Since the focus of this paper is on the laminar regime, we use two-dimensional direct numerical simulation (DNS) for all cases in this paper, which is good enough to reveal the physics of this system. Under the Boussinesq approximation, the non-dimensional governing equations of two-dimensional RB thermal convection is given by

$$\nabla \cdot \boldsymbol{u} = 0, \tag{1}$$

$$\frac{D\boldsymbol{u}}{Dt} = -\nabla P + \frac{1}{\sqrt{Ra/Pr}}\nabla^2 \boldsymbol{u} + \theta \hat{z}, \tag{2}$$

$$\frac{D\theta}{Dt} = \frac{1}{\sqrt{Ra \cdot Pr}}\nabla^2 \theta, \tag{3}$$

where $\boldsymbol{u}$ is velocity, P pressure, θ temperature, and $\hat{z}$ the unit vector of vertical direction. Rayleigh number $Ra = g\beta\Delta\theta H^3/(\upsilon\kappa)$ and Prandtl number $Pr = \upsilon/\kappa$ are the control parameters of this system. All boundaries are non-slip and impermeable. The top and bottom plates are isothermal with fixed temperature $\theta = 0.5$ and $\theta = -0.5$ respectively, while the sidewalls are adiabatic. Staggered grids are used in our simulations. The temporal and spatial discretization schemes have first- and second-order precision respectively. In this paper, the horizontal grids are equidistant, and the vertical grids are refined near boundaries and gaps. The number of grids in the gaps is more than 10 to ensure that the horizontal flows in the gaps are resolved. We choose $Pr = 5.3$, $Ra = 10^7 \sim 2 \times 10^9$, and the width of partition $l = 0.12$. For multi-partition systems, when the number of partitions is large, the influence of the aspect ratio of the convective cell on the flow and heat transfer efficiency is negligible.[16] In order to reduce the CPU time, the aspect ratio Γ is selected as 2 in this paper. For systems with higher Ra number, the more meshes are generally required, so the grid size of the sample with $Ra = 2 \times 10^9$ is tested. By calculating the systems with grid scales of 1000×450 and 2000×900 respectively, it is found that their Nu numbers differ by less than one percent. Therefore, all the samples in this paper are uniformly calculated using the grid scale of 1000×450.

3. Systems with series of d and Ra

In the laminar partitioned RB system, the fluid in each channel moves vertically in alternate directions. Due to the continuity, horizontal flow is formed in the gaps, shearing the thermal boundary layer and transporting the hot/cold fluid to the upward/downward channels. Such process makes the upward/downward channels have higher/lower temperature than the average of the cell, as shown in Fig. 2. This separation between hot upward flow and the cold downward one enhances the global heat transfer effectively. Thus, this "heat-separation" phenomenon is essential to this system. In this section we will focus on the influence of gaps' height d and Ra number over this phenomenon.

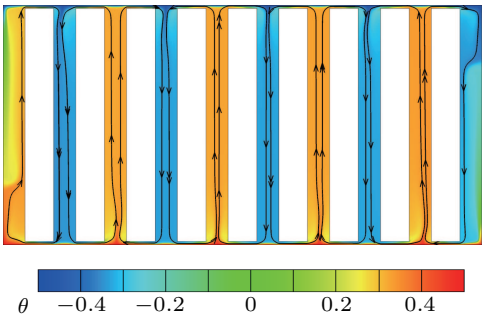


Fig. 2. Temperature field and streamline of partitioned convection system.

We average the temperature in the heat transfer channel in the horizontal direction and then integrate it in the longitudinal direction to obtain the TD number[15] in each heat transfer channels, which represents how strong the heat is separated. The absolute values of TD number in the channels are averaged to get the total TD number of the system, which is able

to reflect the magnitude of temperature drift in the heat transfer channels of the system. The formula for calculating the TD number is expressed as follows:

$$\frac{1}{n+1}\sum_{i=1}^{n+1}\left|\int_0^1 \langle\theta\rangle_{x,i}\mathrm{d}z\right|, \tag{4}$$

where $\langle\ \rangle_{x,i}$ means that the physical quantity in the i-th heat transfer channel is averaged laterally, and n is the number of partitions. Through a series of calculations, the relationships between TD number and height of gaps and Ra number are studied, respectively.

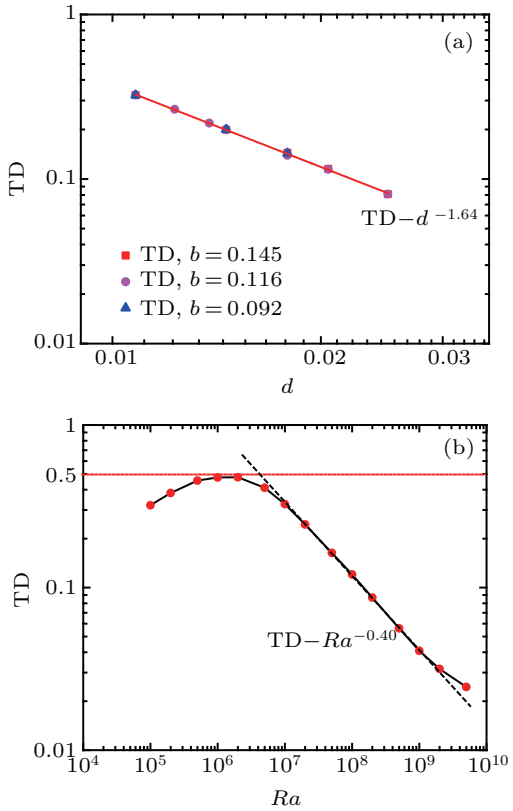


Fig. 3. (a) TD number under various geometric parameters of partitions. (b) TD number with the change of Ra, and the limit value of temperature is 0.5.

Figure 3(a) shows the TD number as a function d at $Ra = 10^8$ with channel width $b = 0.092$, 0.116, and 0.145. Here d ranges from 0.01 to 0.025. We observed a scaling law TD $\sim d^{-1.64}$. The dependence of TD on Ra is shown in Fig. 3(b) with $d = 0.02$ and $b = 0.074$. There are two states in the TD–Ra relation. When Ra is small, TD basically maintains between 0.3 and 0.5, increases gradually and then begins to decline. As Ra increases, it enters the second state, in which TD decreases while Ra increases, and there is a scaling relation between TD and Ra (TD $\sim$Ra$^{-0.40}$). Thus, the TD number varies with d and Ra number, and there are scaling laws with a negative exponent in a certain range of d and Ra.

As mentioned above, the height of gaps is on the same order of magnitude as the thickness of thermal boundary layer. Therefore, the relationship between the height of gaps and the thickness of thermal boundary layer is worth discussing. Zhou *et al.*[22] gave the definition of thickness of thermal boundary layer in turbulent thermal convection. Thickness of thermal boundary layer is defined as the height where the linear fitting line of the temperature near the bottom intersects the horizontally averaged temperature of the bulk region. Two-dimensional RBC system with aspect ratio of 2 has been calculated and Ra number ranges from 10^5 to 10^{10}. Our calculation results show that thickness of thermal boundary layer decreases as Ra increases under a scaling law $\lambda_\theta \sim Ra^{-0.29}$.

We next normalize d in Fig. 3 using the thickness of the thermal boundary layer λ_θ, to reveal the importance of the gap height in the heat separation. We plot the TD number in Fig. 3(a), in which Ra is fixed, together with those in Fig. 3(b), in which d is fixed, as a function of d/λ_θ. It is a surprise to observe that these two sets of results collapse well, as shown in Fig. 4. These results indicate that within a certain parameter range, TD number in the heat transfer channel depends only on the ratio between the gap height d and thermal boundary layer thickness λ_θ.

Therefore, it is necessary to further explore the effect of d/λ_θ on the temperature and heat transfer characteristics of the partitioned RBC.

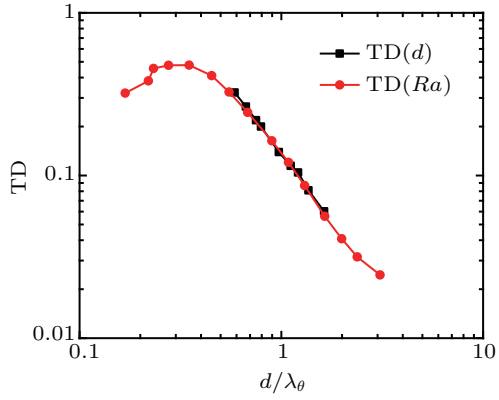


Fig. 4. TD number under different heights of gaps d which are indicated by black solid rectangle and different Ra number which are indicated by red solid circles with the change of d/λ_θ.

4. Effect of d/λ_θ on physical properties of partitioned convective system

We then fixed the thickness of partitions $l = 0.12$, numbers of partitions $n = 8$, the width of channels $b = 0.116$, and Ra changes from 10^7 to 2×10^9. The thickness of thermal boundary layer λ_θ varies with Ra. By changing the height of gaps d, we focus on those cases with $d/\lambda_\theta \approx 0.5$ and $d/\lambda_\theta \approx 1$, and study their temperature distribution and heat transfer.

4.1. Influence of d/λ_θ on TD

First, we focus on the change of TD with *Ra* number under different d/λ_θ.

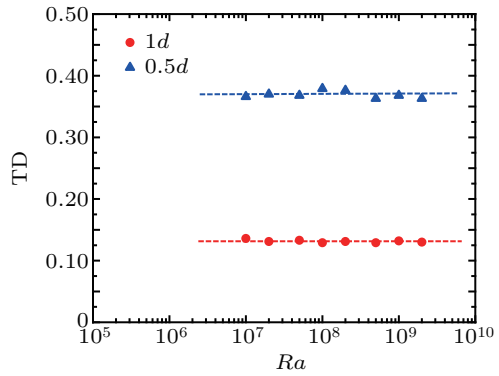


Fig. 5. TD number with the change of *Ra* number when $d/\lambda_\theta \approx 0.5$ or 1. The $1d$ results are indicated by the red solid circles and the $0.5d$ results are indicated by blue solid triangles.

Figure 5 shows TD as a function of *Ra* with fixed d/λ_θ. It can be seen that whether $d/\lambda_\theta \approx 0.5$ or $d/\lambda_\theta \approx 1$. In such cases, TD seems to be independent of *Ra*. TD equals 0.37 when $d/\lambda_\theta \approx 0.5$ and 0.13 when $d/\lambda_\theta \approx 1$. As a quantity reflecting the global temperature distribution property of the system, TD is independent of the aspect ratio of the system and the width of the heat transfer channel. We find that for a given thickness of partitions, TD number depends only on the ratio d/λ_θ, i.e., TD $\sim f(d/\lambda_\theta)$, regardless of *Ra*. This means that the magnitude of d/λ_θ determines the strength of heat separation in this system.

4.2. Temperature distribution near and within the gaps

The gaps and their adjacent area of the partitioned convection system are very close to the thermal boundary layer. Due to the injection of partitions, the thermal boundary layer is suppressed, which is related to the global heat transfer enhancement. In this section we focus on the temperature fields in the gaps and the vicinity at *Ra* equals 10^7, 10^8, and 10^9 and $d/\lambda_\theta \approx 0.5$ or $d/\lambda_\theta \approx 1$. Figure 6 shows the temperature field in the area of and near the lower gap. Figures 6(a), 6(c), and 6(e) correspond to $Ra = 10^7$, 10^8, and 10^9 at $d/\lambda_\theta \approx 0.5$, and figures 6(b), 6(d), and 6(f) correspond to $Ra = 10^7$, 10^8, and 10^9 at $d/\lambda_\theta \approx 1$, respectively. The flows in the gap are all from the cold channels to the hot ones. It is evident in the figure that although the thickness of boundary layer decreases while *Ra* increases, cases with the same d/λ_θ are with similar temperature distribution.

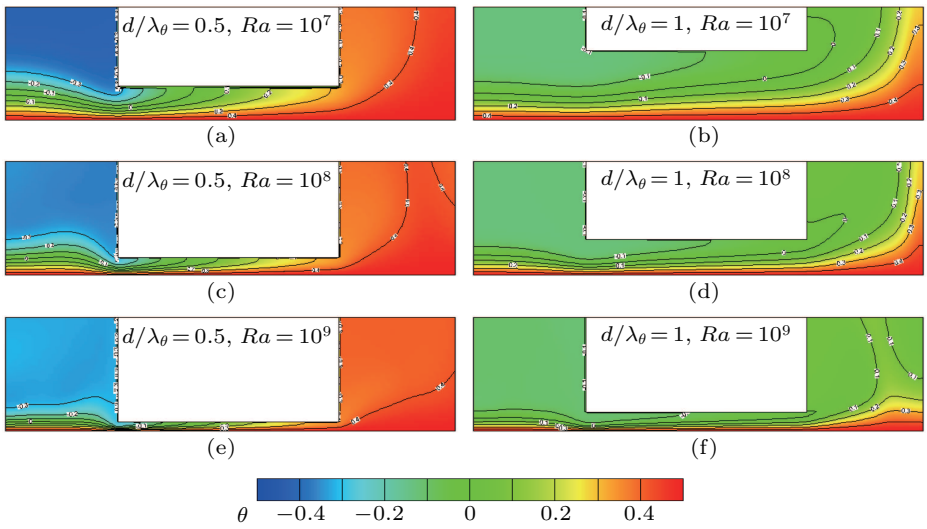


Fig. 6. Temperature field of the gap's area below the fourth partition of the system and the bottom area of the channels adjacent to it. Panels (a), (c), and (e) correspond to $Ra = 10^7$, 10^8, and 10^9 when $d/\lambda_\theta \approx 0.5$. Panels (b), (d), and (f) correspond to $Ra = 10^7$, 10^8, and 10^9 when $d/\lambda_\theta \approx 1$.

From the temperature distribution shown in Figs. 6(a), 6(c), and 6(e), one can see that when the cold fluid passes through the lower gap from left to right, temperature gradually increases due to heating of the bottom plate, and the direction of the gap flow is horizontal. The finest thermal boundary layer is observed at the entrance of the gaps, where the vertical temperature gradient is the largest. The temperature at the outlet is between 0.3 and 0.4. The temperature of fluid at the bottom of the right channel is also between the two isotherms whose values are equal to 0.3 and 0.4. Since d/λ_θ is fixed, the height of the gap is different between *Ra* numbers. However, their temperatures of the fluid entering the right channels are close, and the heating processes of the fluid in the gaps by the bottom plates are also similar. In Figs. 6(b)–6(d), the flows are similar to the former series, except that the fluid has not been heated completely when they flow through the gaps, which may be caused by larger heights of the gaps. Also, there is still cold fluid in the upper part of the gaps. Thus, the temperature of the fluids exiting the gaps ranges from 0.1 to 0.2, which is lower than that of the $d/\lambda_\theta \approx 0.5$ cases.

To show the similarity of these cases, we again normalized the heights of the gaps by the thickness of the boundary layer, and the temperature distributions under different *Ra* in the gaps are discussed in details. Three temperature contours $\theta = 0.1$, 0.2, and 0.3 with $d/\lambda_\theta \approx 0.5$ are extracted from the results shown in Figs. 6(a), 6(c), and 6(e), and presented in Fig. 7(a). The gray rectangular in the figure is the region where the partition is located. Figure 7(b) is the result of $d/\lambda_\theta \approx 1$, in which three temperature contours of -0.1, 0, and 0.1 are selected.

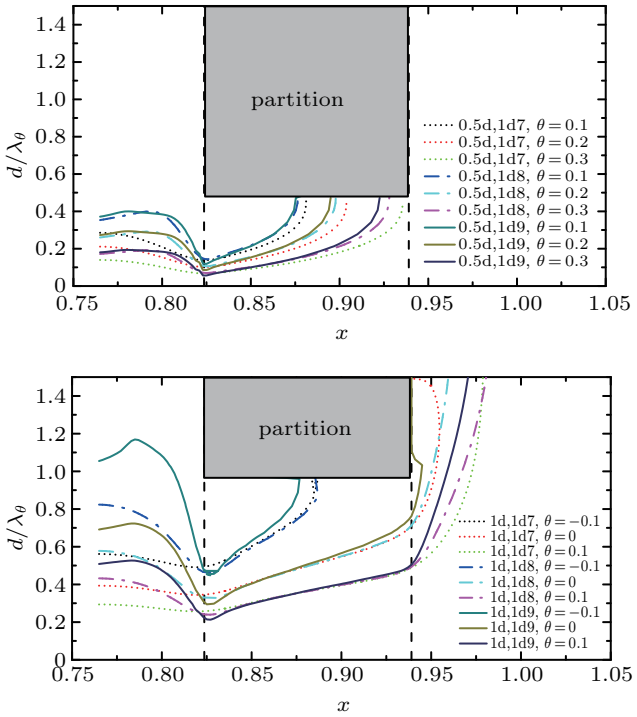


Fig. 7. When $d/\lambda_\theta \approx 0.5$, three isotherms of 0.1, 0.2, and 0.3 are selected (a) and $d/\lambda_\theta \approx 1$, three isotherms of -0.1, 0, and 0.1 are selected (b) at $Ra = 10^7$ (dots), $Ra = 10^8$ (dash Dot), and $Ra = 10^9$ (solid). The gray area in the figure is the area where the partition is located.

Figure 7 convinces that the temperature distribution in the gap is similar when d/λ_θ is the same, also the fluid is under similar heating process when passing through the gap. As shown in Fig. 7(a), when $d/\lambda_\theta \approx 0.5$, the isotherms are divided into two regions. Before entering the gaps, the isotherms basically horizontal. Upon approaching the gap, the heights of isotherms gradually decrease, reaching the lowest position at the entrance. After entering the gap, three isotherms gradually rise and end at the bottom of the partition, and the thickness of the thermal boundary layer also increases. In Fig. 7(b), when $d/\lambda_\theta \approx 1$, the isotherms are divided into three regions. Before entering the gap, the isotherms of different *Ra* vary greatly, but they all reach the lowest point at the entrance of the gap. After entering the gap, the isotherms of the same temperature value for different *Ra* numbers almost collapse, and the height rises gradually. The isotherms of -0.1 end up at the bottom of the partition, and the isotherms of 0.0 and 0.1 can extent out of the gap.

In a word, the thickness of the thermal boundary layer of different *Ra* numbers varies greatly, but as long as d/λ_θ are the same, the distributions of temperature in the gaps are basically the same.

4.3. Effect of d/λ_θ on *Nu* number

As shown in the previous section, in the partitioned convection, we find that for the same d/λ_θ, the same TD will be produced. In the last part of this section, we will again focus on the effect on heat transfer efficiency, which is the widespread interest in this field.

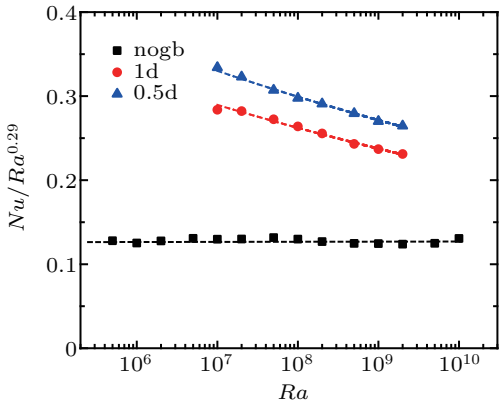


Fig. 8. Semi-log plot of $Nu/Ra^{0.29}$ as functions of *Ra*. $0.5d$ ($d/\lambda_\theta \approx 0.5$) and $1d$ ($d/\lambda_\theta \approx 1$) are indicated by blue solid triangle and red solid circles, respectively. nogb ($Nu/Ra^{0.29}$ of system without partitions) are indicated by black solid rectangle. The dash lines represent the best power-law fits of corresponding cases.

Figure 8 shows change of *Nu* with *Ra* for the two series of simulations, together with *Nu* in the non-partitioned convection system as a comparison. As shown in Fig. 8, for $d/\lambda_\theta \approx 0.5$ and $d/\lambda_\theta \approx 1$, *Nu* is much higher than the case without partitions, which is an example of the heat transfer enhancement in the partitioned convection system. Within the given range of *Ra*, the maximum heat transfer efficiency enhancement happens at $Ra = 10^7$, whose *Nu* is 2.2 times of the non-partitioned one for $d/\lambda_\theta \approx 1$, and 2.6 times for $d/\lambda_\theta \approx 0.5$. With the increase of *Ra*, the enhancement of heat transfer efficiency decreases gradually. We also observed a scaling relation between *Nu* and *Ra* for both $d/\lambda_\theta \approx 0.5$ and 1, which yields $Nu \sim Ra^{0.25}$. Even though, the enhancement effect in the partitioned convection is still huge. The smallest heat transfer efficiency at $Ra = 2 \times 10^9$ for $d/\lambda_\theta \approx 1$ is nearly twice as large as that without partitions.

5. Conclusion

A series of studies have been carried out on the physical characteristics of the partitioned convection system. Because the height of the gaps is usually selected within the thickness of thermal boundary layer of RB convection, the characteristics of temperature drift characteristics in the partitioned con-

vection system are studied in detail for a given thickness of partitions $l = 0.12$, and the following conclusions are obtained.

(i) By using the thickness of thermal boundary layer to normalize the height of gaps, TD numbers of different gaps' heights or different *Ra* numbers are analyzed, and it is found that the curves of these two changes with d/λ_θ coincide basically.

(ii) The ratio of gaps' heights to thickness of thermal boundary layer is selected as constant value, and it is found that TD numbers have nothing to do with *Ra* numbers, and TD ≈ 0.37 when $d/\lambda_\theta \approx 0.5$, TD ≈ 0.13 when $d/\lambda_\theta \approx 1$.

(iii) Even if the thermal boundary layer will change with different *Ra* number, the temperature distributions of the gap and its adjacent area are basically the same when the d/λ_θ are fixed under different *Ra* numbers.

(iv) Under the same *Ra* number, the heat transfer efficiency of systems when $d/\lambda_\theta \approx 0.5$ is higher than that of the systems when $d/\lambda_\theta \approx 1$. With a given magnitude of d/λ_θ, there is a scale relationship between *Nu* number and *Ra* number, $Nu \sim Ra^{0.25}$.

Acknowledgment

The authors thank Ding G Y for useful discussion and advices.

References

[1] Lappa M 2005 *Cryst. Res. Technol.* **40** 531
[2] Ahlers G, Grossmann S and Lohse D 2009 *Rev. Mod. Phys.* **81** 503
[3] Bodenschatz E, Pesch W and Ahlers G 2000 *Annu. Rev. Fluid. Mech.* **32** 709
[4] Xia K Q 2013 *Theor. Appl. Mech. Lett.* **3** 052001
[5] Du Y B and Tong P 1998 *Phys. Rev. Lett.* **81** 987
[6] Wei P, Chan T S, Ni R, Zhao X Z and Xia K Q 2014 *J. Fluid Mech.* **740** 28
[7] Joshi P, Rajaei H, Kunnen R P J and Clercx H J 2017 *J. Fluid Mech.* **830** R3
[8] Kunnen R P, Clercx H J and Geurts B J 2006 *Phys. Rev. E* **74** 056306
[9] Kooij G L, Botchev M A and Geurts B J 2015 *Int. J. Heat & Fluid Flow* **55**
[10] Weiss S, Wei P and Ahlers G 2016 *Phys. Rev. E* **93** 043102
[11] Guzman D N, Xie Y, Chen S, Rivas D F, Sun C, Lohse D and Ahlers G 2016 *J. Fluid Mech.* **787** 331
[12] Cheng J P, Zhang H N, Cai W H, Li S N and Li F C 2017 *Phys. Rev. E* **96** 013111
[13] Cheng J P, Cai W H, Zhang H N, Li F C, Shen L and Qian S Z 2019 *Physics of Fluids* **31** 023105
[14] Bao Y, Chen J, Liu B F, She Z S, Zhang J and Zhou Q 2015 *J. Fluid Mech.* **784** R5
[15] Bao Y, Lin Z P and Ding G Y 2017 *Computer Aided Engineering* **26** 57 (in Chinese)
[16] Lin Z P and Bao Y 2018 *Sci. Sin. Phys. Mech. & Astron.* **48** 054702
[17] Lin Z P and Bao Y 2018 *Sci. Sin. Phys. Mech. & Astron.* **48** 104702 (in Chinese)
[18] Bao Y and Lin Z P 2019 *Sci. Sin. Phys. Mech. & Astron.* **49** 044701 (in Chinese)
[19] Hajmohammadi M R 2018 *Int. J. Refrigeration* **88** 16
[20] Fugmann H, Di Lauro P, Sawant A and Schnabel L 2018 *Energies* **11** 1322
[21] Xue Y, Ge Z, Du X and Yang L 2018 *Energies* **11** 1398
[22] Zhou Q, Stevens R J A M, Sugiyama K, Grossmann S, Lohse D and Xia K Q 2010 *J. Fluid Mech.* **664** 297